Autotuning of Decentralized and Centralized PID Control Systems for Non-Square Systems

Priyadharsini. M.; Kalpana, D.* [+]
Department of Instrumentation Engineering, MIT Campus, Anna University, Chennai, INDIA

Chidambaram, M.
Department of Chemical Engineering, National Institute of Technology, Warangal, Telangana, INDIA

ABSTRACT: *This paper presents a systematic procedure to obtain the decentralized and centralized PID controller settings for a non-square stable Multi-Input and Multi-Output (MIMO) system using a simultaneous relay autotuning method with the incorporation of higher-order harmonics. In general, the assumption of filtering the higher-order harmonics will be acceptable when the system has the characteristics of a low-pass filter. However, higher-order harmonics have an impact on the controller parameter evaluation and it needs attention. Therefore, this research addresses the control of non-square stable MIMO systems in their original non-square form instead of squaring them by adding or deleting variables, and also the significance of higher-order harmonics in non-square stable MIMO systems is considered. To enhance the controller performance, higher-order harmonics are taken into consideration by observing the initial dynamics of the relay response. The decentralized and centralized control systems performances are explored by simulation on two different 3 inputs and 2 outputs models with different levels of interactions. For these models, simulation studies were carried out for both servo and regulatory operations. The performance of the centralized control system is improved for systems with interaction (relative gain is more than 1) by 18-41% for servo operation and 14-31% for regulatory operation. Also, the performance is improved for decentralized controllers for systems with a relative gain of less than one. The time integral analysis comparison between centralized and decentralized control schemes with the incorporation of higher-order harmonics using the simultaneous relay autotuning method is implemented. The effectiveness and performance of the proposed scheme are also analyzed even in the presence of robustness and the effect of measurement noise.*

KEYWORDS: *Non-square system; Decentralized controllers; Centralized controllers; Relay autotuning; Higher-order harmonics.*

INTRODUCTION

By using the relay autotuning method, the ultimate period (P_u) and ultimate gain (K_u) can be determined for single input single output (SISO) systems. By using the tuning formula of Ziegler Nichols' continuous cycling method, the PID controller settings are calculated and presented in [1]. Excellent analysis of relay autotuning methods is discussed in [2], [3], and [4].

In a SISO system, there is only one critical point,

***** *To whom correspondence should be addressed.*
+ *E-mail: kalpanaspec@gmail.com*
1021-9986/2023/2/577-600 24/$/2.04

however, in a MIMO system, there are more critical points. Hence, it can produce the limit cycles that are described as stability limits as discussed in [5]. A relay feedback test is conducted by replacing the decentralized and centralized controllers with relays. The sustained oscillations in the relay response have the identical period as the SISO system with lower frequency and it is proved in [6] and [7]. As described in [5], the relative magnitudes (h1, h2) remain unchanged. For identifying the critical points, the relay autotuning method is mostly utilized.

For SISO systems, the relay feedback test is substitute for the conventional continuous cycling method to get sustained oscillations of the system and compute the ultimate gain and ultimate frequency is proposed in [8]. For a highly nonlinear distillation column, autotuning variation is extended in [9]. A full closed-loop test for relay feedback autotuning methods for stable, integrating, and unstable processes is proposed in [10]. The relay feedback used to identify general model structures using the state-space approach is discussed in [11]. From the relay feedback test, the shape information is analyzed to evaluate the accurate model structure of the process and develop conditions for stability of continuous cycling of limit cycles for low-order systems is implemented in [12]. The low- order modeling of a system using the relay feedback responses is proposed in [13]. For first, second, third, and higher-order processes, derived time domain analytical expression for the relay response are discussed in [14]. The derivation of relay responses expression using biased relay in the time domain and identification algorithms are proposed in [15]. For a first-order plus time delay transfer function model, an asymmetrical relay feedback method is modified for improved system identification is proposed in [16]. For nonlinear processes, a relay feedback test is used for identifying a wiener model is implemented in [17].

For MIMO systems, processes may be square or non-square types. The process with the same value of a manipulated and controlled variable is referred as a square system, and different values of manipulated and controlled variables are referred as a non-square system. The sequential identification using relay feedback method is used to identify the model parameters of a MIMO stable square system using ideal relays implemented as in [18]; which was extended to higher dimensional square systems given in [19]. Derived analytical expressions for a 2×3 non-square MIMO system using the sequential relay autotuning procedure and model parameter estimation are proposed in [20]. However, the above techniques do not estimate the ultimate parameters (K_u and P_u) of the unknown system very accurately. From the literature, it is observed that for a non-square stable MIMO system, the importance of higher-order harmonics and the methodology to incorporate the effects are not addressed.

Non-square systems with an uneven number of inputs and outputs are frequently experienced in the chemical industry's processes. A few examples of such systems are the mixing tank process discussed by [21], the Shell standard control problem investigated by [22], the crude distillation unit presented by [23], etc. A comparison of the IMC controller for a 2×3 non-square system is presented in [24]. For multivariable non-square systems, a new method using Internal Model Control (IMC) to design a Smith delay compensation decoupling controller with a first-order time-delay transfer function is presented in [25]. The decoupling internal model controller for a non-square stable process with multiple time delays is presented in [26]. The CRONE (Commande Robuste d'Ordre Non-Entier) controller is designed for a non-square multivariable air-path system of a turbocharged diesel engine is discussed in [27]. A full matrix centralized PI controller for a high dimensional multivariable system based on an equivalent transfer function is proposed in [28]. The design of the V-norm internal model controller for a non-square system is proposed in [29]. An extended version of the Davison method with a pseudo-inverse for the steady-state gain matrix is used to design centralized multivariable PI controllers in the Smith delay compensator is implemented in [30]. For a non-square system, a predictive PI controller is proposed in [31]. The control of unstable systems with multivariable PI controllers is discussed in [32]. The design of decentralized controllers using relay autotuning for unstable TITO systems with time delays is implemented in [33].

The decentralized controller is designed by the independent IMC design procedure for non-square systems is discussed in [34]. The control of the non-square system with the sequential relay autotuning method is implemented in [20]. The modeling and control of under-defined and over-defined non-square systems are implemented for a complex non-linear chemical process using sequential relay feedback test is discussed in [35]. The decentralized controller is designed for non-square unstable MIMO systems using the simultaneous relay autotuning method is given in [36]. To obtain the settings of the decentralized PI controller, simultaneous relay autotuning is employed for a non-square stable MIMO system, and the effects of higher-order harmonics are analyzed in [37]. The centralized PID controllers are designed using the simultaneous relay auto-tuning method for non-square 2×3 unstable transfer function matrix. The importance of higher-order harmonics is analyzed in [38].

Generally, the Higher-Order Harmonics (HOH) are not filtered out from the output of all the systems during the relay feedback test. This assumption will be applicable if the system displays a low-pass filter characteristic. The existence of Higher-order harmonics can affect critical point computation. Hence, higher-order harmonic analysis is required for determining the controller parameters. The existence of HOH is determined by the sustained oscillation of relay response, and the improved ultimate gain (K_u) value is calculated using the appropriate method. It is important to note that incorporating higher-order harmonics only affects the system's controller gains and has no effect on derivative time or integral time as discussed in [4]. The improved controller gain appears to be detuned values. Determination of controller parameters without using the relay autotuning method could take a long time and be difficult.

The main contribution of this paper is the simultaneous relay autotuning of decentralized and centralized PID controls of two non-square stable Multi-Input and Multi-Output (MIMO) systems with the incorporation of higher-order harmonics. Higher-order harmonics are analyzed from the sustained oscillation of the relay response, and PID controllers are designed with improved ultimate gain for both decentralized and centralized control schemes. The closed-loop studies are investigated for servo and regulatory operations with time integral analysis. The effect of measurement noise and robustness shows better performance with the incorporation of higher-order harmonics. The design of decentralized PID controller for mild interaction system and centralized controller for high interaction system with the consideration of higher-order harmonics for evaluating the critical points using the simultaneous autotuning method for non-square stable MIMO systems is addressed in this paper.

Accordingly, the paper is organized as follows: In the theoretical section, preliminaries and design procedures for decentralized and centralized PID control schemes by incorporating higher-order harmonics using the simultaneous autotuning method are discussed. In the next section, simulation studies on non-square MIMO stable systems are presented. Following the simulation studies, the robustness studies and the effect of measurement noise are presented. Concluding remarks are presented at the end.

THEORETICAL SECTION

Here, the two non-square MIMO systems are considered for analysis with different levels of interactions. The decentralized and centralized controllers are designed by replacing the controllers by relays and conducted the simultaneous relay autotuning test. When an unknown system is excited (by small amount) with an ideal/ biased relay of height ‘h’ in a closed-loop situation, the output starts oscillating around its set/steady value and the system shows limit cycles of amplitude ‘a’ with a period of P_u. The output lags behind the input by pi radians. The ultimate properties of the system become ultimate frequency (ω_u) and ultimate gain K_u which may be given as: $K_u=4*h/(pi*a)$ and $\omega_u=2*pi/P_u$. In PID autotuning based on relay feedback, these ultimate properties are used for controller settings. The PID controller parameters are evaluated by the proper selection of tuning procedures. Similarly, relay autotuning using the simultaneous relay autotuning method is employed to design a decentralized and centralized PID control system as discussed in [4].

Preliminaries

The notations listed below are used for 2×3 MIMO systems:

The process matrix is given by Eq. (1).

$$G_p(s)=\begin{pmatrix} G_{p11}(s) & G_{p12}(s) & G_{p13}(s) \\ G_{p21}(s) & G_{p22}(s) & G_{p23}(s) \end{pmatrix} \quad (1)$$

The decentralized controller and centralized controller transfer function matrix are given by Eq. (2) and (3), respectively.

$$G_c(s)=\begin{pmatrix} G_{c1}(s) & 0 \\ G_{c2}(s) & 0 \\ 0 & G_{c3}(s) \end{pmatrix} \quad (2)$$

$$G_c(s) = \begin{pmatrix} G_{c11}(s) & G_{c12}(s) \\ G_{c21}(s) & G_{c22}(s) \\ G_{c31}(s) & G_{c32}(s) \end{pmatrix} \quad (3)$$

The manipulated input variables and output variables are given by Eqs. (4) and (5).

$$u(s) = \begin{pmatrix} u_1(s) \\ u_2(s) \\ u_3(s) \end{pmatrix} \quad (4)$$

$$(s) = \begin{pmatrix} y_1(s) \\ y_2(s) \end{pmatrix} \quad (5)$$

The output of all the systems during the relay feedback test does not filter out the higher-order harmonics. When the system has a low-pass filter characteristic, in that case, the assumption will be applicable. The occurrence of higher-order harmonics can affect the calculation of the critical points. Analysis of higher-order harmonics is needed while evaluating the controller parameters. From the output relay response, the presence of HOH is analyzed and the appropriate technique is used to compute the ultimate gain (K_u) value. Or else, it has an effect on the estimation of the ultimate gain. The method recommended by [3] is extended here to non-square stable MIMO systems.

Sustained relay oscillations are similar to a triangular waveform, it is expressed by Eq. (6).

$$y(t^*) = a^*\left[1 + \frac{1}{3^2} + \frac{1}{5^2} + \frac{1}{7^2} + \cdots + \frac{1}{N^2} + \cdots\right] \quad (6)$$

Sustained relay oscillations are similar to a rectangular waveform, it is expressed by Eq. (7).

$$y(t^*) = a^*\left[1 - \frac{1}{3} + \frac{1}{5} - \frac{1}{7} + \cdots + \frac{1}{N} + \cdots\right] \quad (7)$$

The approximate value of HOH is recommended as a≅0.909y (t) when the waveform is neither triangular nor rectangular. By observing the initial dynamics and HOH occurrence of the relay response, an appropriate N value is selected and the y(t*) is recorded at time $t^*=0.5\pi/\omega_u$. The improved values of a* are acquired by solving equations (6) and (7), respectively. It is important to remember that, a* is not the value of amplitude directly obtained from the relay response.

An appropriate number of HOH terms can be preferred depending on the initial dynamics of the relay output response. It should also be highlighted that including all the higher-order harmonic elements may cause inaccuracy in the determination of the ultimate values. As a result, determining the ultimate gains needs an accurate evaluation.

The block diagram of decentralized and centralized control scheme for 2×3 non-square system are shown in Fig. 1 and Fig. 2, respectively.

The ZN continuous cycling method is employed to design all controllers for a stable system and it is listed in Table 1.

Design Procedure

1- Identify the steady-state gain of the appropriate paired system.

2- Conduct the simultaneous relay feedback test by replacing the relays with the proper switching signs instead of the controllers, as shown in Fig. 1 and Fig. 2, respectively.

3- The critical points are obtained from the sustained oscillations of the relay response.

4- Consider the existence of higher-order harmonics in the sustained oscillations of the relay response.

5- Determine the improved ultimate gain, with the incorporation of higher-order harmonics using Eq. (6).

6- Design the PID controllers for the stable systems using the tuning rule given in Table.1.

7- Compare decentralized and centralized controller performance quantitatively and qualitatively.

8- Analyze the effect of measurement noise and the robustness of the designed controllers.

Simulation studies on non-square MIMO stable system

Model 1

The following system matrix is considered from [32] and it is suitably modified as given in Eq. (8).

$$G(s) = \begin{bmatrix} \frac{1.6667\, e^{-s}}{(1.6667s+1)} & \frac{0.42e^{-s}}{(1.6667s+1)} & \frac{e^{-s}}{(1.6667s+1)} \\ \frac{0.8333\, e^{-s}}{(1.6667s+1)} & \frac{0.21e^{-s}}{(1.6667s+1)} & \frac{1.6667e^{-s}}{(1.6667s+1)} \end{bmatrix} \quad (8)$$

The inverse of the steady state gain matrix for the above process is given by Eq. (9).

$$K_p^{-1} = \begin{bmatrix} 0.8059 & -0.4835 \\ 0.2031 & -0.1218 \\ -0.4285 & 0.8571 \end{bmatrix} \quad (9)$$

The RGA of the above process is calculated as given by Eq. (10).

Table 1: ZN continuous cycling tuning rules.

Controller	$K_{C,des}$	τ_I	τ_D
P	$0.5K_{u,max}$	-	-
PI	$0.45K_{u,max}$	$0.833P_u$	-
PID	$0.6K_{u,max}$	$0.5P_u$	$0.125P_u$

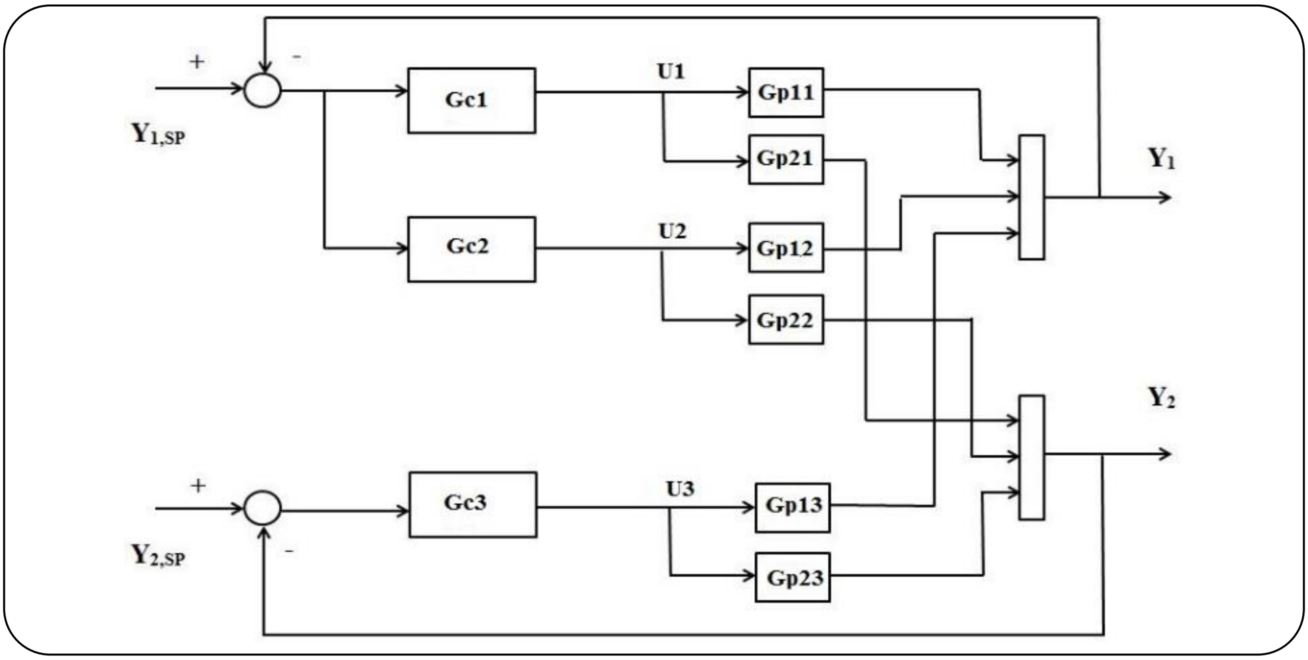

Fig. 1: Block diagram of 2×3 decentralized control system

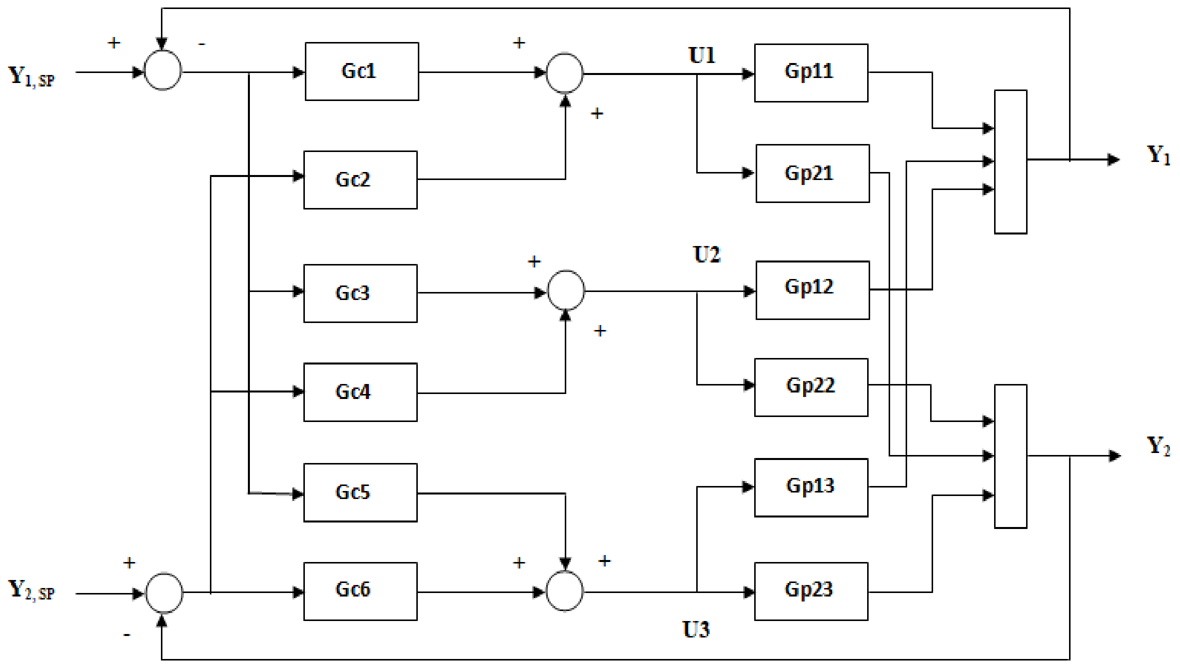

Fig. 2: Block diagram of 2×3 centralized control system.

$$RGA = \Lambda = K_p \times [K_p^{-1}]' \tag{10a}$$

$$\Lambda = \begin{bmatrix} 1.3432 & 0.0853 & -0.4285 \\ -0.4029 & -0.0256 & 1.4285 \end{bmatrix} \tag{10b}$$

Here, [ ]' denotes the transpose of a matrix and × denotes element-by-element multiplication. For this Model 1, the interaction of this system is large, as seen from Equation (10b). The proper pairing of the input and the output variables is found by applying the block relative gain (BRG) implemented in [21]. For this Model 1, equation (10b) indicates that y1 is to be paired with u1 and u2; and y2 is to be paired with u3. For the decentralized configuration, the relays are connected as follows:

$$\begin{bmatrix} u_1(s) \\ u_2(s) \\ u_3(s) \end{bmatrix} = \begin{bmatrix} R_1(s) & 0 \\ R_2(s) & 0 \\ 0 & R_3(s) \end{bmatrix} \begin{bmatrix} e_1(s) \\ e_2(s) \\ e_3(s) \end{bmatrix} \tag{11}$$

For the centralized configuration, the relays are connected as follows:

$$\begin{bmatrix} u_1(s) \\ u_2(s) \\ u_3(s) \end{bmatrix} = \begin{bmatrix} R_1(s) & R_4(s) \\ R_2(s) & R_5(s) \\ R_3(s) & R_6(s) \end{bmatrix} \begin{bmatrix} e_1(s) \\ e_2(s) \\ e_3(s) \end{bmatrix} \tag{12}$$

Decentralized controller

The decentralized PID controllers are designed using the simultaneous relay autotuning method, according to the design procedure, and the sustained oscillation measurements are given in Table 2. The a_1 and a_2 are the amplitudes of the y1 relay response, and a_3 is the amplitude of the y2 relay response. The sustained oscillation of relay response for Model 1 obtained from decentralized control design is shown in Fig. 3. It can be seen that the sustained oscillation of the relay response is triangular in shape with the absence of initial dynamics. Hence, the controllers are designed without improving the ultimate gain.

The ultimate gain and controller parameters for the decentralized controller are listed in Table 3.

Centralized controller

The centralized PID controllers are designed using the simultaneous relay autotuning method, according to the design procedure, and the sustained oscillation measurements are given in Table 4. The a_1, a_2, and a_3 are the amplitudes of the y1 relay response, and the a_4, a_5, and a_6 are the amplitudes of the y2 relay response. Fig.4.depicts the sustained oscillation of the relay response

Table 2: Results using Relay feedback test of decentralized control design (Model 1).

h_1	h_2	h_3	a_1	a_2	a_3	P_u
0.16	0.04	0.16	0.2	0.2	0.18	3.3

Table 3: Ultimate gain and controller parameters of the decentralized controller (Model 1).

	Ku	KC	KI	KD
Gc,11	1.0186	0.61116	0.3707	0.2521
Gc,21	0.2546	0.15276	0.0926	0.0630
Gc,32	1.1318	0.67908	0.4116	0.2801

τ_I = 1.65; τ_D = 0.4125

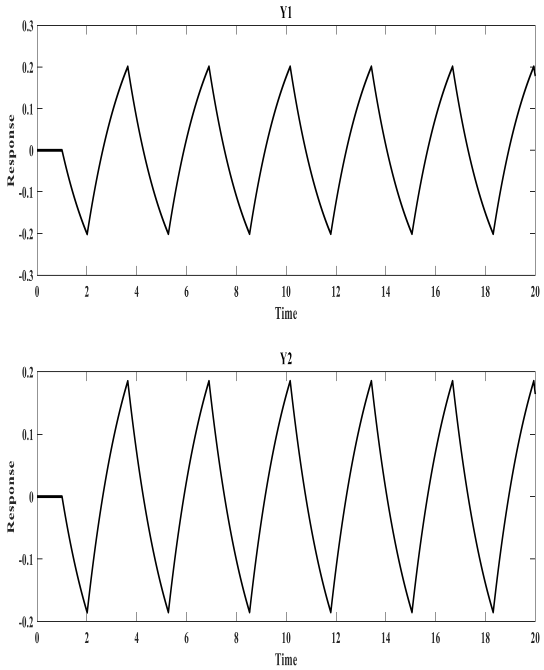

Fig. 3: Sustained oscillation of relay test for Decentralized control design (Model 1).

of Model 1 obtained from centralized control design. The sustained oscillation of the relay response is triangular in shape with no initial dynamics. As a result, the controllers are not designed with improved ultimate gain.

The ultimate gain and controller parameters for the centralized controller are displayed in Table 5.

The servo response and the regulatory response of Model 1 for decentralized and centralized control systems are presented in Fig.5 and 6, respectively. For regulatory

Table 4: Results using relay feedback test of centralized control design (Model 1).

h_1	h_2	h_3	h_4	h_5	h_6	a_1	a_2	a_3	a_4	a_5	a_6	P_u
0.16	-0.08	0.04	-0.02	-0.1	0.16	0.092	0.092	0.092	0.078	0.078	0.078	3.3

Table 5: Ultimate gain and controller parameters for centralized controller (Model 1).

	K_u	K_C	K_I	K_D
$G_{c,11}$	2.2143	1.32858	0.8052	0.5480
$G_{c,12}$	-1.1.72	-0.66432	-0.4026	-0.2740
$G_{c,21}$	0.0554	0.03324	0.0202	0.0137
$G_{c,22}$	-0.3265	-0.1959	-0.1187	-0.0808
$G_{c,31}$	-1.6324	-0.97944	-0.5936	-0.4040
$G_{c,32}$	2.6118	1.56708	0.9497	0.6464

τ_I = 1.65; τ_D = 0.4125

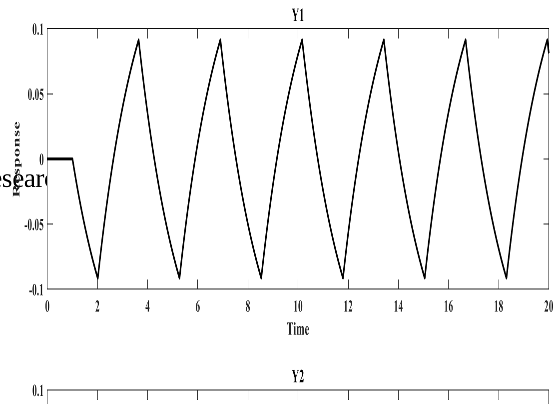

Fig. 4: Sustained oscillation of relay test for centralized control design (Model 1).

problem, the load variable enters the system along with the manipulated variable. It is observed from the response that, the centralized control system exhibits a significant enhancement in performance.

For servo and regulatory operations, the quantitative evaluation of the centralized controller with the decentralized controller is evaluated by using the time-integral performance analysis, and it is shown in Tables 6 and 7, respectively.

From Tables 6 and 7, it is inferred that the centralized controllers have less sum of ISE values than the decentralized controller. For the servo problem, there is a percentage refinement in ISE values of about 18% and 29% in the process curve, whereas the interaction curve is improved by 19%, 19%, and 22%. From the evaluation, it is inferred that, for a highly interactive system, the centralized control system gives improved performance than the decentralized control system. Also, it is observed from the Fig. 5 and 6 that, the centralized PID controller response gives less settling time, reduced system interaction and enhanced performance.

Model 2

Consider the transfer function matrix of mixing tank with 3 inputs and 2 outputs by [21] by adding the delay of 30% as given in Eq. (13).

$$G(s) = \begin{bmatrix} \dfrac{4\,e^{-6s}}{20s+1} & \dfrac{4e^{-6s}}{20s+1} & \dfrac{4e^{-6s}}{20s+1} \\ \dfrac{3\,e^{-3s}}{10s+1} & \dfrac{-3e^{-3s}}{10s+1} & \dfrac{5e^{-3s}}{10s+1} \end{bmatrix} \tag{13}$$

The inverse of the steady state gain matrix is given by Eq. (14).

$$K_p^{-1} = \begin{bmatrix} 0.0673 & 0.0385 \\ 0.1394 & -0.1346 \\ 0.0433 & 0.0962 \end{bmatrix} \tag{14}$$

Table 6: Control performance analysis for servo response (Model 1).

Controller	Response (Y1)			Interaction (Y2)			Interaction (Y1)			Response (Y2)			Sum of ISE
	ISE	IAE	ITAE	ISE	IAE	ITAE	ISE	IAE	ITAE	ISE	IAE	ITAE	
Decentralized	1.366	2.184	4.02	0.2239	1.05	3.507	0.352	1.316	4.395	1.324	2.09	3.71	3.2659
Centralized	1.205	1.655	2.16	0.1068	0.51	1.291	0.057	0.374	0.940	1.141	1.55	1.8	2.5098

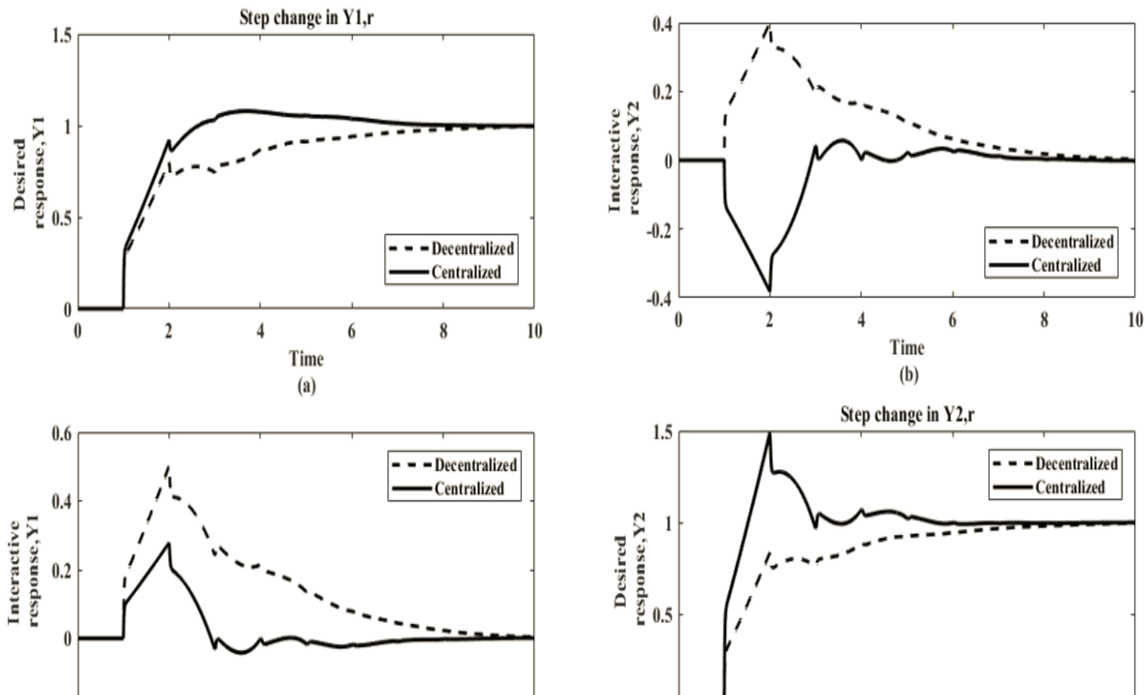

Fig. 5: Process and interaction curve of servo responses (Model 1)

The RGA of the above process is calculated as given by Eq. (15).

$$\mathrm{RGA} = \Lambda = \mathrm{K_p} \times \left[\mathrm{K_p}^{-1}\right]' \qquad (15a)$$

$$\Lambda = \begin{bmatrix} 0.2692 & 0.5577 & 0.1731 \\ 0.1154 & 0.4038 & 0.4808 \end{bmatrix} \qquad (15b)$$

Here, [ ]' denotes the transpose of a matrix and × denotes element-by-element multiplication. The block relative gain (BRG) is used to find the block diagonal model and the input-output pairings are presented in [21]. For this Model 2, y_1 is paired with u_1 and u_2; and y_2 is paired with u_3.

Decentralized controller

The decentralized PID controllers are designed using the simultaneous relay autotuning method, according to the design procedure, and the sustained oscillation measurements are given in Table 8. The a_1 and a_2 are the amplitudes of the y1 relay response, and a_3 is the amplitude of the y2 relay response. Fig. 7 shows the sustained oscillation of the relay response for Model 2 obtained from the decentralized control design. It is observed that the sustained oscillation of the relay response is triangular in shape with the absence of initial dynamics. Hence, the controllers are designed without improving the ultimate gain.

Table 7: Control performance analysis for regulatory response (Model 1).

Step change	Controller	Y1			Y2			Sum of ISE
		ISE	IAE	ITAE	ISE	IAE	ITAE	
d1	Decentralized	1.505	2.631	8.972	0.2297	1.147	4.826	1.7347
	Centralized	1.033	1.948	5.855	0.369	1.231	3.999	1.402
d2	Decentralized	0.09557	0.663	2.261	0.01459	2.889	1.216	0.1101
	Centralized	0.06561	0.491	1.475	0.02343	0.3102	1.008	0.0890
d3	Decentralized	0.2884	1.27	5.469	1.424	2.524	8.47	1.7124
	Centralized	0.269	0.8858	2.367	0.843	1.654	4.651	1.112

Table 8: Results using Relay feedback test of decentralized control design (Model 2).

h_1	h_2	h_3	a_1	a_2	a_3	P_{u1}	P_{u2}	P_{u3}
0.3	0.3	0.3	0.62	0.62	0.39	20	20	11

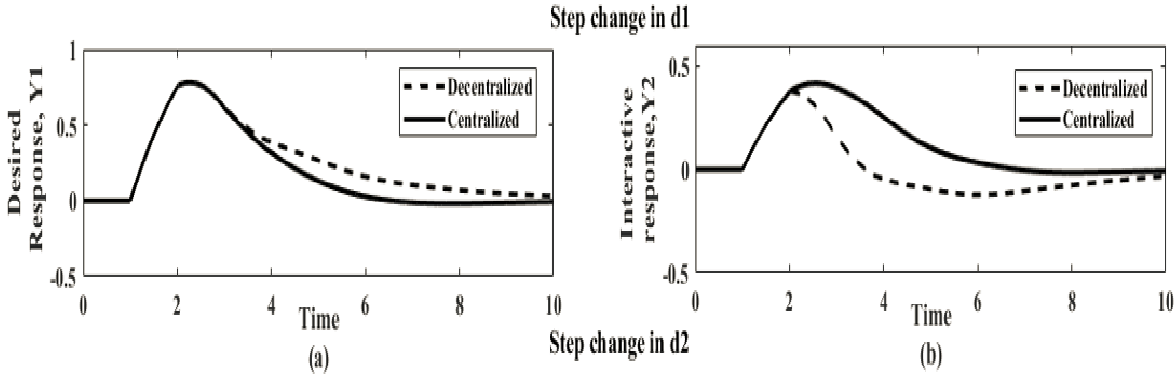

Fig. 6: Process and interaction curve of regulatory responses (Model 1).

Table 9: Ultimate gain and controller parameters of the decentralized controller (Model 2).

	K_u	K_C	K_I	K_D
$G_{c,11}$	0.6161	0.36966	0.03697	0.92415
$G_{c,21}$	0.6161	0.36966	0.03697	0.92415
$G_{c,32}$	0.9794	0.58764	0.10684	1.4691

τ_{I1}= 10; τ_{I2}= 5.5; τ_{D1} = 2.5; τ_{D2} = 1.375

Table 10: Results using relay feedback test of centralized control design (Model 2)

h_1	h_2	h_3	h_4	h_5	h_6	a_1	a_2	a_3	a_4	a_5	a_6	P_u
0.4	0.3	0.4	-0.3	0.4	0.3	0.95	0.95	0.95	1.35	1.35	1.35	18

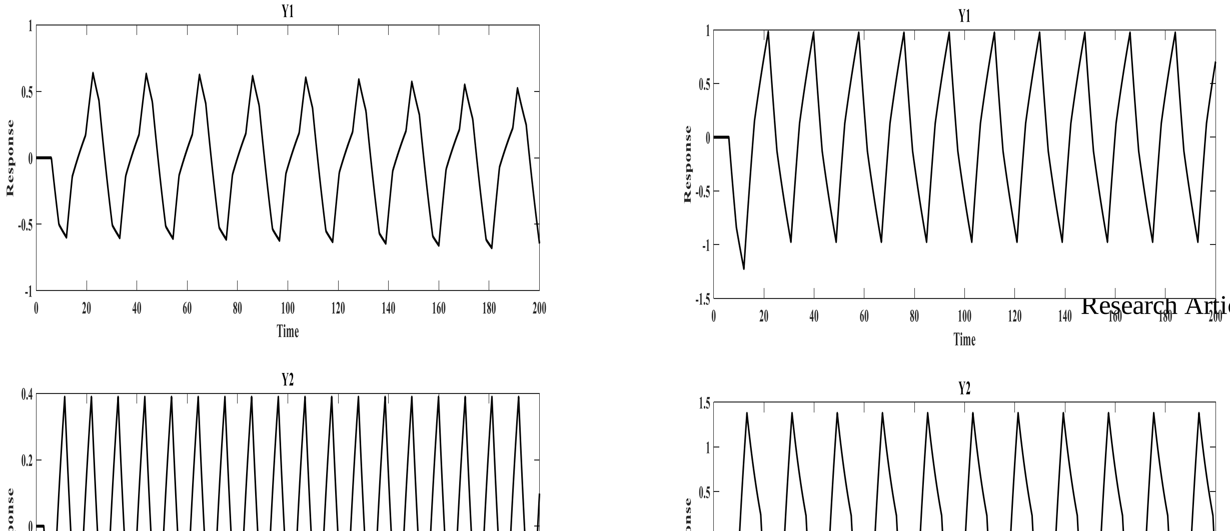

Fig. 7: Sustained oscillation of relay test for decentralized control design (Model 2).

Fig. 8: Sustained oscillation of relay test for centralized control design (Model 2).

The ultimate gain and controller parameters for the decentralized controller are given in Table 9.

Centralized controller

The centralized PID controllers are designed using the simultaneous relay autotuning method, according to the design procedure, and the sustained oscillation measurements are given in Table 10. The a_1, a_2 and a_3 are the amplitudes of the y1 relay response, and the a_4, a_5, and a_6 are the amplitudes of the y2 relay response. Fig. 8 depicts the sustained oscillation of the relay response of Model 2 obtained from centralized control design. The plant model offers insufficient filtering, and it is analyzed from the relay output response. From the initial dynamics of the relay response in Fig.8, a value of N=3, 1 is preferred.

The ultimate gain and controller parameters for the centralized controller are given in Table 11.

The servo response and the regulatory response of Model 2 for decentralized and centralized control systems are presented in Fig.9 and 10, respectively. It is observed from the response that, both decentralized and centralized

Table 11: Ultimate gain and controller parameters for centralized controller (Model 2).

	K_u	K_C	K_I	K_D	y(t*)	a*(N=3,1)	K_u*	K_C*
$G_{c,11}$	0.5361	0.32166	0.03574	0.72374	0.8	0.72	0.7074	0.42444
$G_{c,12}$	0.4021	0.24126	0.02681	0.54284	0.8	0.72	0.5305	0.3183
$G_{c,21}$	0.5361	0.32166	0.03574	0.72374	0.8	0.72	0.7074	0.42444
$G_{c,22}$	-0.2829	-0.16974	-0.01886	-0.38192	1	1	-0.38197	-0.22918
$G_{c,31}$	0.3773	0.22638	0.02515	0.50936	1	1	0.5093	0.30558
$G_{c,32}$	0.2829	0.16974	0.01886	0.38192	1	1	0.38197	0.22918

τ_I = 9; τ_D = 2.25; ω_u= 0.3491; t=4.499*

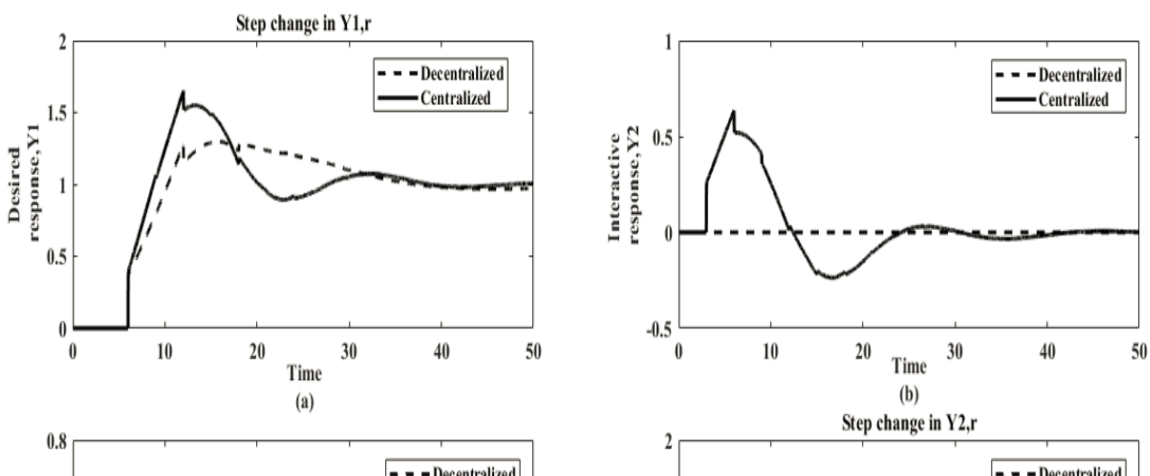

Fig. 9: Process and interaction curve of servo response (Model 2).

control systems exhibit a better performance in servo and regulatory operations.

For servo and regulatory operations, the quantitative evaluation of the decentralized controller and the centralized controller is evaluated by using performance analysis, and it is shown in Tables 12 and 13, respectively.

From Tables 12 and 13, in the process curve of servo response, it is inferred that, there is a percentage refinement of ISE value, 41% for the decentralized controller in loop 1 and 30% for the centralized controller in loop 2. The interaction curve is improved by 28% for the decentralized controller, 14% for the centralized controller and 31% for the decentralized controller. Also, the decentralized controllers have less sum of ISE values than the centralized controller. From the evaluation, it is inferred that, for a less interactive system, the decentralized controller outperforms the centralized controller.

Table 12: Control performance analysis for servo response (Model 2).

Controller	Response (Y1)			Interaction (Y2)			Interaction (Y1)			Response (Y2)			Sum of ISE
	ISE	IAE	ITAE	ISE	IAE	ITAE	ISE	IAE	ITAE	ISE	IAE	ITAE	
Decentralized	7.592	12.22	134.6	0	0	0	1.82	5.969	101.4	3.679	6.158	47.74	13.091
Centralized	8.144	11.84	110.4	1.796	5.415	65.26	0.393	2.393	33.74	3.465	5.513	38.82	13.798

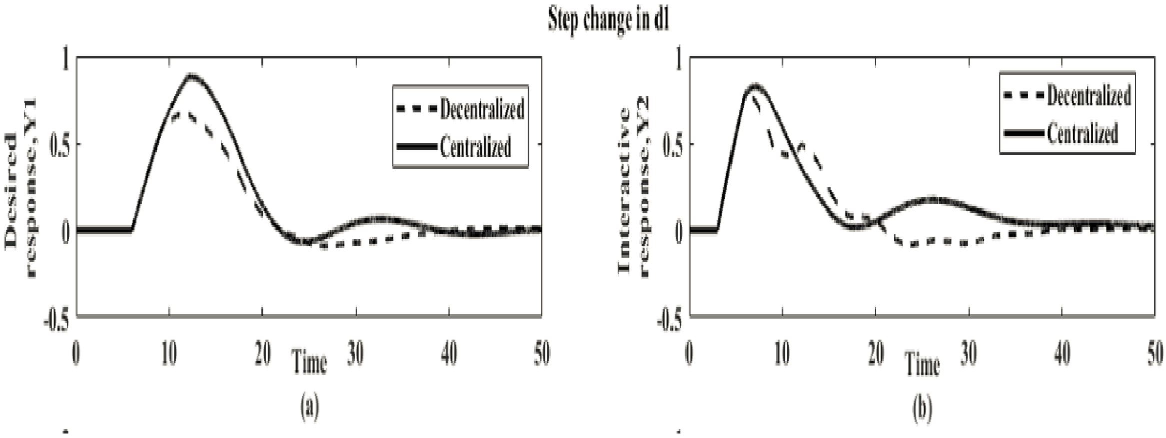

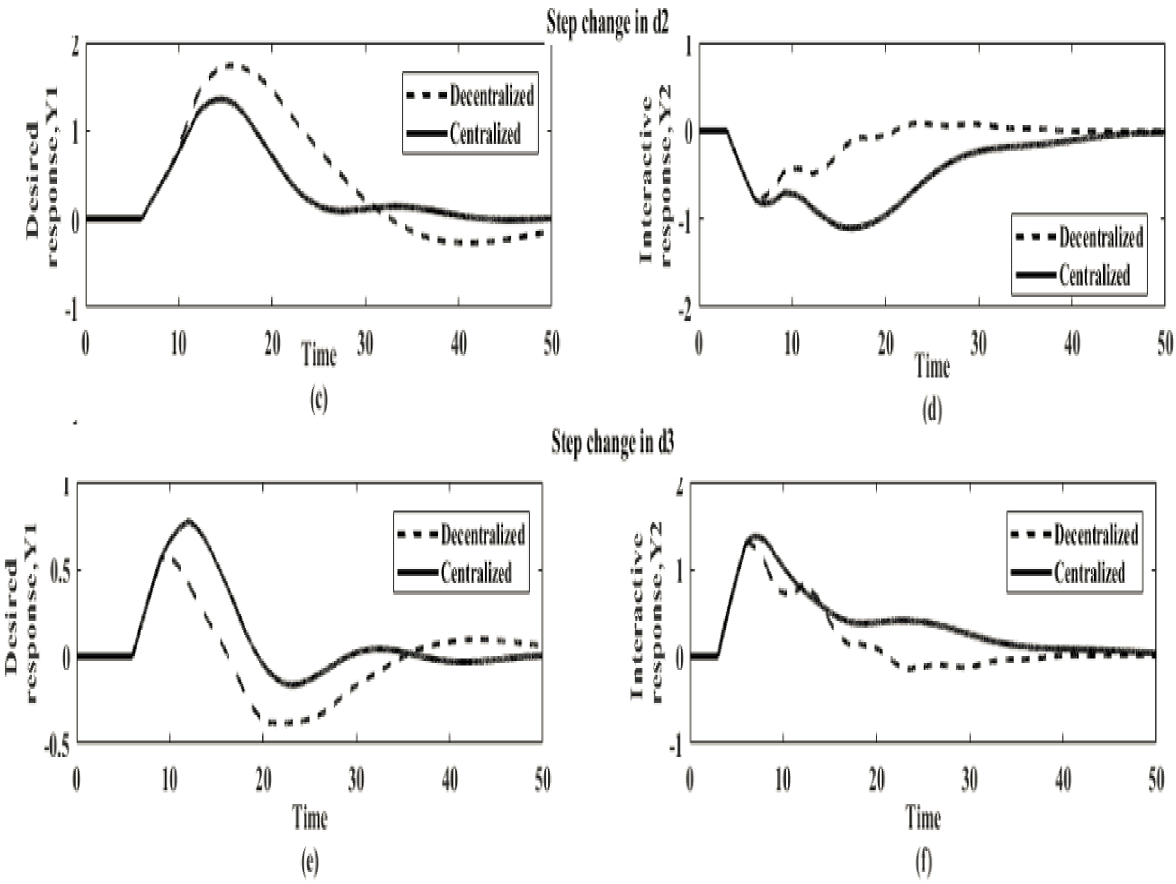

Fig. 10: Process and interaction curve of regulatory response (Model 2).

Table 13: Control performance analysis for regulatory response (Model 2).

Step change	Controller	Y1			Y2			Sum of ISE
		ISE	IAE	ITAE	ISE	IAE	ITAE	
d1	Decentralized	3.261	7.189	109.6	3.281	7.284	87.9	6.542
	Centralized	5.263	8.752	131.2	3.875	8.456	124.8	9.138
d2	Decentralized	33.37	28.64	591.8	3.281	7.284	87.9	36.651
	Centralized	15.02	16.47	280	16.51	21.69	388.7	31.53
d3	Decentralized	2.834	8.846	189.7	9.115	12.14	146.5	11.949
	Centralized	3.696	7.508	114.2	13.55	18.5	296	17.246

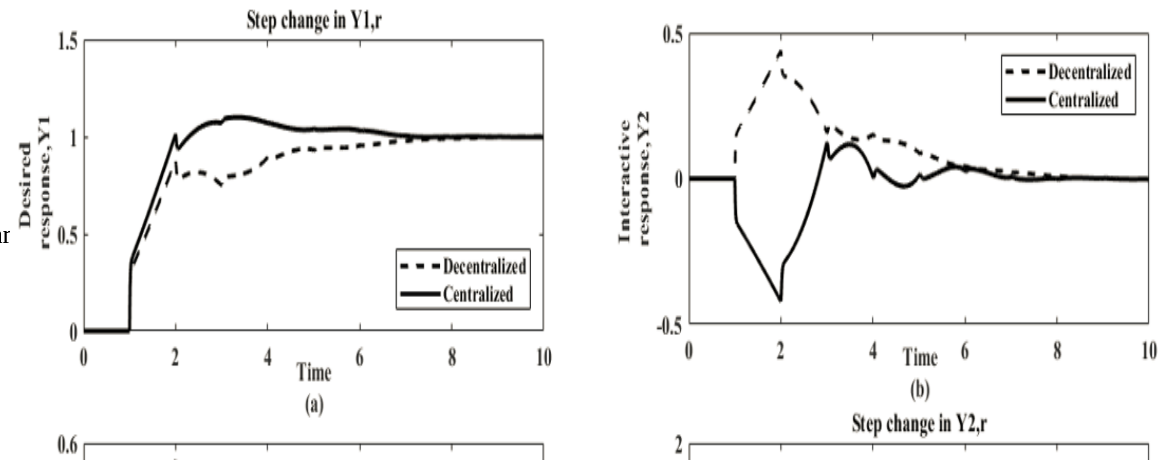

Fig. 11: Process and interactions curve with +10% gain perturbation (Model 1)

Robustness analysis

The robustness of the systems is determined by the perturbation uncertainties of individual element gain of the transfer function model by ±10% without varying the controller settings of the MIMO non-square system.

Model 1

The servo response and the regulatory response of Model 1 for decentralized and centralized control systems with ±10% gain perturbation are presented in Fig.11 and 12, respectively.

The servo responses of a ±10% perturbed system gives the less settling time, reduced system interaction, and improved performance as shown in Fig.11& 12, respectively.

The time-integral analysis is performed for decentralized and centralized controllers for servo operations with ±10% perturbations in the system and it is listed in Table 14 and 15, respectively.

Table 14: Control performance analysis for servo response with ±10% of perturbation (Model 1).

	Controller	Response (Y1)			Interaction (Y2)			Interaction (Y1)			Response (Y2)			Sum of ISE
		ISE	IAE	ITAE	ISE	IAE	ITAE	ISE	IAE	ITAE	ISE	IAE	ITAE	
+10%	Decentralized	1.294	1.996	3.268	0.2215	0.9635	2.923	0.3482	1.208	3.663	1.259	1.91	3.009	3.1227
	Centralized	1.167	1.58	1.951	0.1284	0.5888	1.489	0.06807	0.4287	1.084	1.194	1.659	2.123	2.5574
+10%	Decentralized	1.459	2.404	4.944	0.2308	1.147	4.219	0.3628	1.438	5.285	1.411	2.301	4.569	3.4636
	Centralized	1.259	1.768	2.468	0.09384	0.4882	1.283	0.04974	0.3554	0.9338	1.119	1.543	1.87	2.5215

Table 15: Control performance analysis for regulatory response with ±10% of perturbation (Model 1).

Step change	Controller	Y1			Y2			Sum of ISE
		ISE	IAE	ITAE	ISE	IAE	ITAE	

Perturbation of +10% in all process gain								
d1	Decentralized	1.277	2.511	8.946	0.2229	1.099	4.57	1.4999
	Centralized	1.11	1.939	5.575	0.397	1.228	3.815	1.507
d2	Decentralized	0.08104	0.6325	2.254	0.01415	0.2768	1.151	0.09519
	Centralized	0.07046	0.4885	1.405	0.02521	0.3094	0.9615	0.09567
d3	Decentralized	0.321	1.319	5.485	1.221	2.405	8.38	1.542
	Centralized	0.269	0.8858	2.367	0.8425	1.654	4.651	1.1115
Perturbation of -10% in all process gain								
d1	Decentralized	1.097	2.45	9.292	0.1795	1.019	4.519	1.2765
	Centralized	0.956	1.951	6.141	0.3405	1.229	4.173	1.2965
d2	Decentralized	0.06968	0.6175	2.341	0.0114	0.2568	1.139	0.0810
	Centralized	0.06071	0.4917	1.547	0.02163	0.3097	1.052	0.08234
d3	Decentralized	0.2585	1.223	5.423	1.05	2.353	8.726	1.3085
	Centralized	0.2472	0.8952	2.525	0.7776	1.663	4.909	1.0248

From Tables 14 and 15, it is observed that, for the highly interactive system, the centralized controller gives improved performance than the decentralized controller. The centralized controllers have less sum of ISE values than the decentralized controller with ±10% perturbations in the system. Also, the centralized controller is more robust than the decentralized controller.

Model 2

The servo responses and the regulatory response of Model 2 for decentralized and centralized control systems with ±10% perturbed systems are shown in Fig. 13 & 14, respectively.

The servo responses of a ±10% perturbed system give better performance in desired response and interactive response, as shown in Fig.13 & 14, respectively. The time-integral analysis is performed for decentralized and centralized controllers for servo operations with ±10% perturbations in the system and it is shown in Tables 16 and 17, respectively.

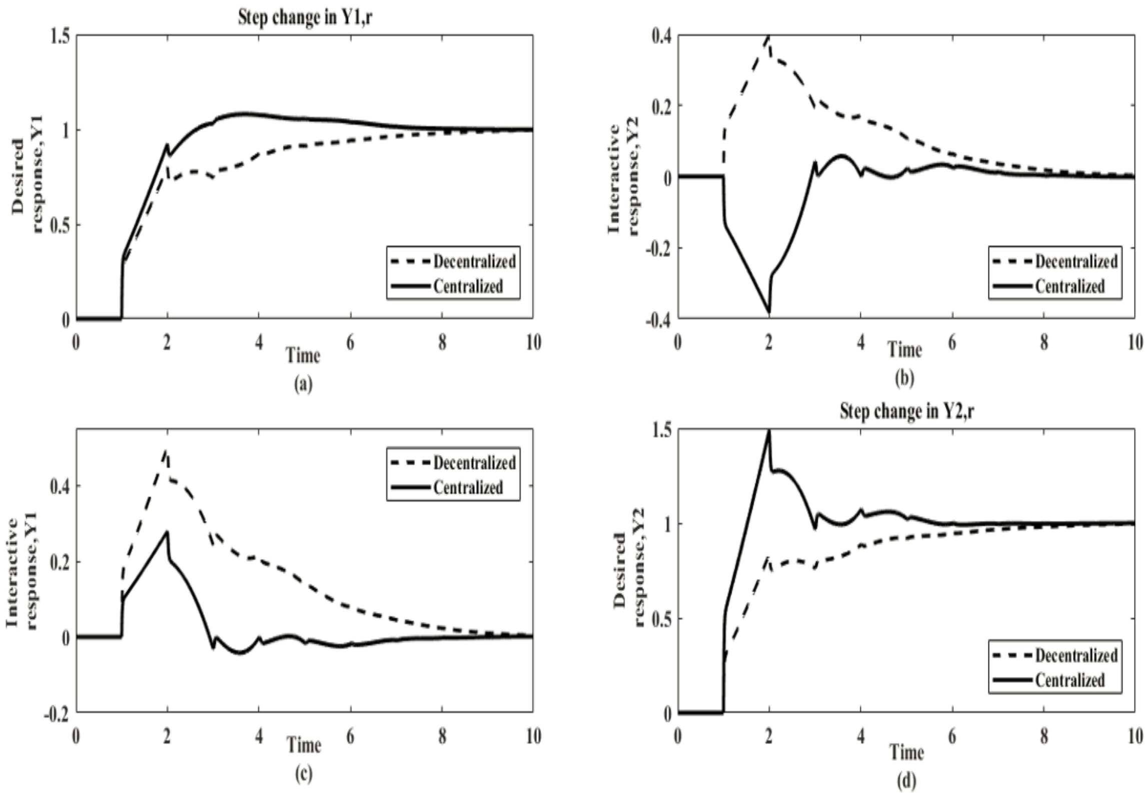

Fig. 12: Process and interactions curve with -10% gain perturbation (Model 1).

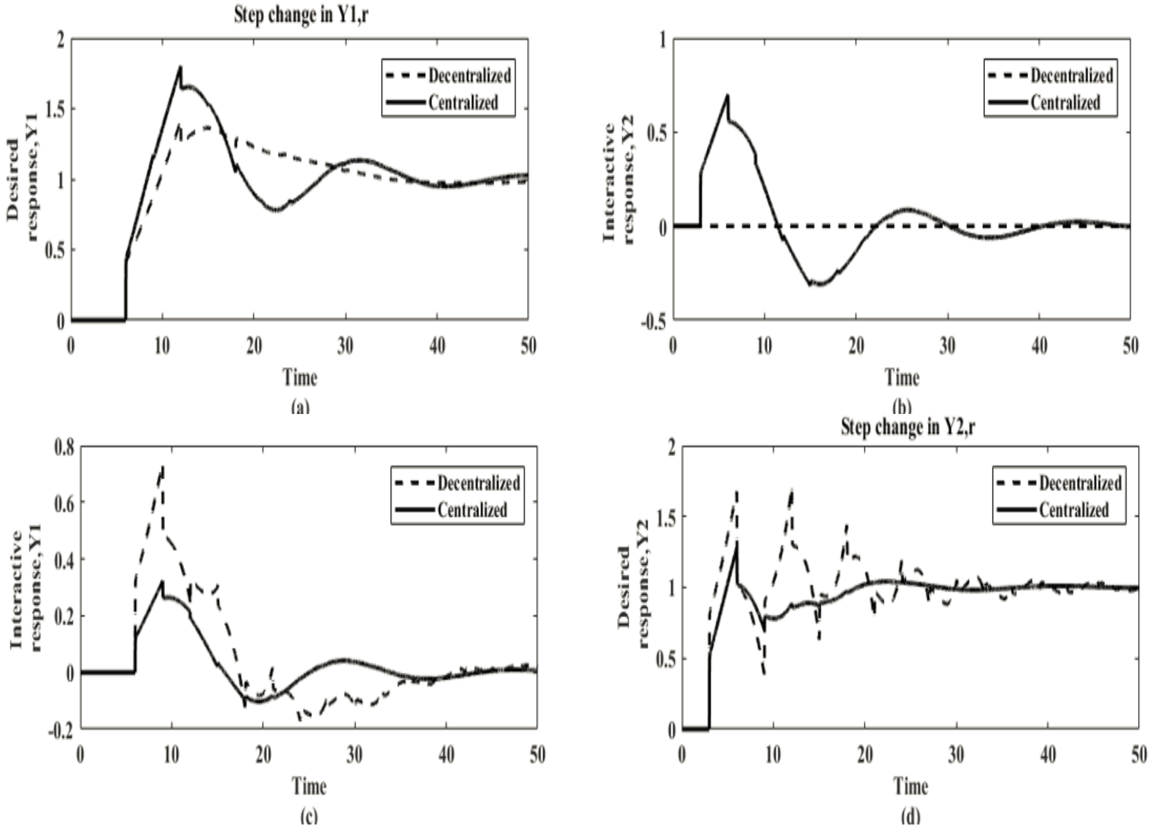

Fig. 13: Process and interactions curve with +10% gain perturbation (Model 2).

Table 16: Control performance analysis for servo response with ±10% perturbation (Model 2)

	Controller	Response (Y1)			Interaction (Y2)			Interaction (Y1)			Response (Y2)			Sum of ISE
		ISE	IAE	ITAE	ISE	IAE	ITAE	ISE	IAE	ITAE	ISE	IAE	ITAE	
+10%	Decentralized	7.587	11.97	124.1	0	0	0	1.846	5.862	95.92	4.293	7.858	83.63	13.726
	Centralized	8.871	13.33	146.9	2.131	6.309	85.15	0.4462	2.758	43.44	3.434	5.552	36.76	14.882
-10%	Decentralized	7.694	12.48	144.9	0	0	0	1.853	6.449	116	3.444	5.759	42.42	12.991
	Centralized	7.697	10.92	89.58	1.554	5.002	58.68	0.3594	2.162	28.22	3.58	5.78	33.59	13.19

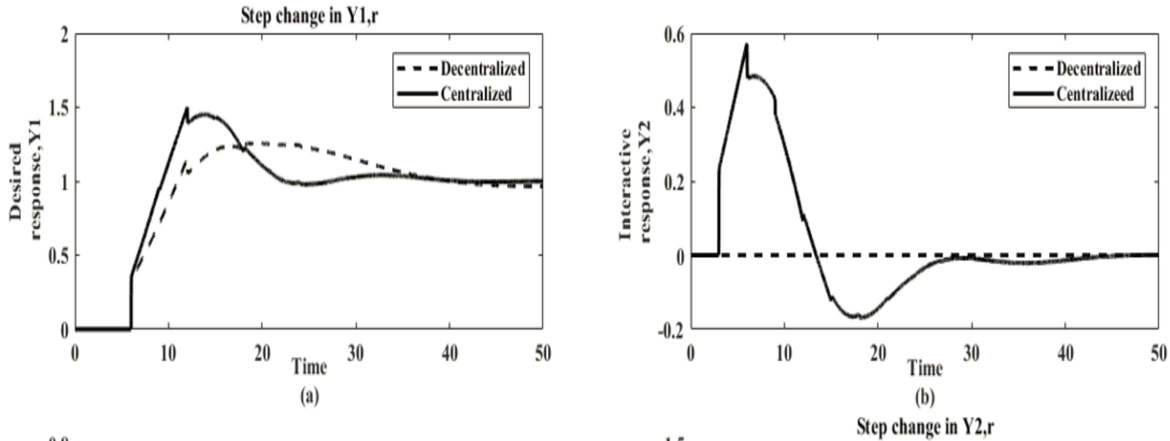

Fig. 14: Process and interactions curve with -10% gain perturbation (Model 2).

From Tables 16 and 17, it is observed that, for the less interactive systems, the decentralized controller is more robust than the centralized controller. The servo performances of the decentralized controller have less sum of ISE values than the centralized controller, with ±10% perturbations in the system. Also, the decentralized controller is more robust than the centralized controller.

Effect of measurement noise

The impact of measurement noise plays a crucial part in analyzing the performance of the controllers. While conducting the relay feedback test, a measurement noise of zero mean and 0.0005 variance is added to the output variable.

Model 1

Decentralized controller

The sustained oscillation of Model 1 in the presence of noise obtained from decentralized control design is shown in Fig.15.

Table 17: Control performance analysis for regulatory response with ±10% of perturbation (Model 2).

Step change	Controller	Y1			Y2			Sum of ISE
		ISE	IAE	ITAE	ISE	IAE	ITAE	
Perturbation of +10% in all process gain								
d1	Decentralized	3.459	7.145	104.8	3.479	7.313	87.08	6.938
	Centralized	5.82	9.655	154.6	4.175	8.552	125.5	9.995
d2	Decentralized	35.4	28.28	559.1	3.479	7.313	87.08	38.879
	Centralized	16.59	16.71	282	17.51	21.65	374.1	34.1
d3	Decentralized	3.03	8.807	182.7	9.665	12.19	145.1	12.695
	Centralized	4.131	8.429	138.2	14.22	18.56	291	18.351
Perturbation of -10% in all process gain								

d1	Decentralized	3.076	7.269	115.5	3.123	7.317	91.31	6.199
	Centralized	4.813	8.256	120.1	3.617	8.413	125.8	8.43
d2	Decentralized	31.26	28.64	613.8	3.123	7.317	91.31	34.383
	Centralized	13.71	16.46	289	15.56	21.69	404.3	29.27
d3	Decentralized	2.653	8.755	192.2	8.676	12.2	152.2	11.329
	Centralized	3.357	7.045	105.2	12.9	18.45	302.5	16.257

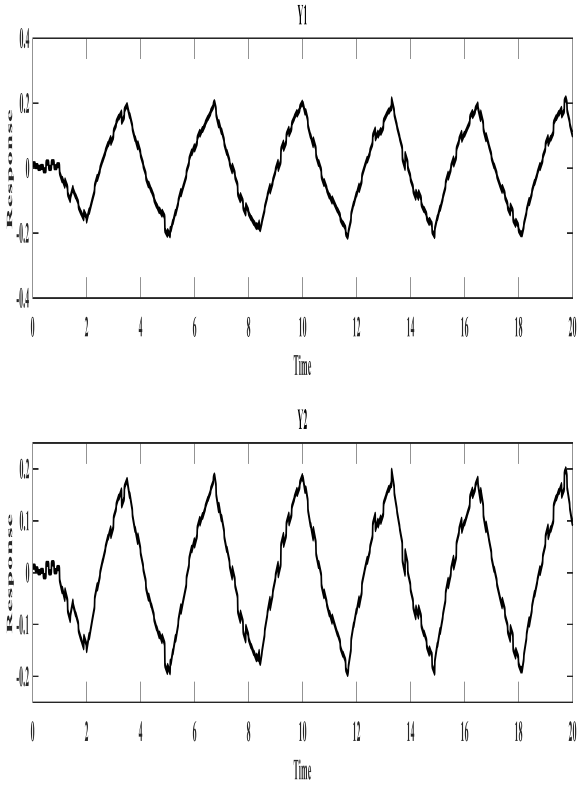

Fig. 15: Relay responses for decentralized control design in presence of random noise (Model 1).

The sustained oscillation of Model 1 in the presence of noise obtained from decentralized control design is shown in Fig.15.

Centralized controller

The output of the relay response in the presence of random noise obtained from the centralized control design is shown in Fig. 16.

The results obtained from the sustained oscillation of the relay response are listed in Table 20. The PID controller parameters for centralized controllers are designed using the measurements acquired from the relay responses are listed in Table 21.

Fig.17. shows the process and interaction curve for the servo responses in the occurrence of the noise with a mean of 0 and variance of 0.0005 for the decentralized and centralized controller. The servo responses of a system gives less settling time, reduced system interaction and improved performance even in the presence of noise, is shown in Fig.17.

The controller performance analysis of servo response with noise for Model 1 is listed in Table 22.

From Table 22, it is observed that, there is an improvement in the performance analysis of the

Table 18: Relay feedback test results for decentralized control design with noise (Model 1).

h_1	h_2	h_3	a_1	a_2	a_3	P_u
0.16	0.04	0.16	0.1963	0.1963	0.1811	3.26

Table 19: PID Controller parameters for decentralized controller with noise (Model 1).

	K_u	K_C	K_I	K_D
$G_{c,11}$	1.0377	0.6226	0.3819	0.2537
$G_{c,21}$	0.2594	0.15566	0.0954	0.06342
$G_{c,32}$	1.1248	0.6749	0.4140	0.2750

$\tau_I = 1.63$; $\tau_D = 0.4075$

Table 20: Relay feedback test results for centralized control design with noise (Model 1).

h1	h2	h3	h4	h5	h6	a1	a2	a3	a4	a5	a6	Pu
0.16	-0.08	0.04	-0.02	-0.1	0.16	0.0905	0.0905	0.0905	0.077	0.077	0.077	2.99

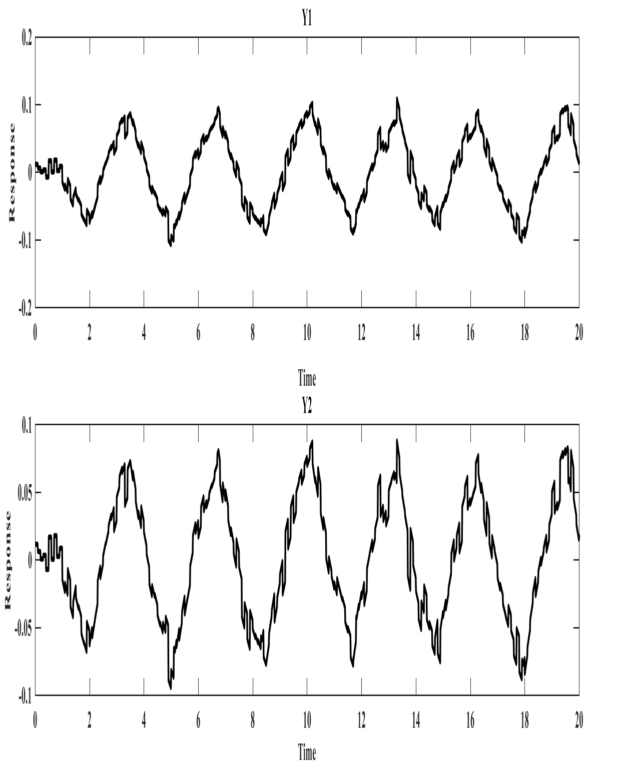

Fig. 16: Relay responses for centralized control design in presence of random noise (Model 1).

centralized control system, which have less sum of ISE value than the decentralized control system with the existence of noise.

Model 2

Decentralized controller

The sustained oscillation of Model 2 in the occurrence of noise obtained from decentralized control design is shown in Fig.18.

The results obtained from the sustained oscillation of the relay response are listed in Table 23. Table 24 lists the controller parameters for decentralized controllers with noise.

Centralized controller

The output of the relay response in the presence of random noise obtained from the centralized control design is shown in Fig.19.

The results obtained from the sustained oscillation of the relay response are displayed in Table 25.

The initial dynamics are observed from the relay response in Fig.19, a value of N=3, 1 is selected. The PID controller parameters for centralized controllers are designed using the measurements acquired from the relay responses are listed in Table 26.

Fig.20. shows the process and interaction curve for the servo responses in the occurrence of the noise with a mean of 0 and variance of 0.0005 for the decentralized and centralized controllers. The servo responses of a system shows reduced system interaction and improved performance even in the presence of noise as shown in Fig.20.

Table 21: PID controller parameters for Centralized Controller with noise (Model 1).

	K_u	K_C	K_I	K_D
$G_{c,11}$	2.2510	1.3506	0.9034	0.5047
$G_{c,12}$	-1.1255	-0.6753	-0.4517	-0.2523
$G_{c,21}$	0.5627	0.3376	0.2258	0.1261
$G_{c,22}$	-0.3307	-0.1984	-0.1327	-0.07414
$G_{c,31}$	-1.6535	-0.9921	-0.6636	-0.3707
$G_{c,32}$	2.6456	1.5874	1.0618	0.5932

$\tau_I = 1.495;\ \tau_D = 0.3737$

Table 22: Control performance analysis of servo response with noise (Model 1).

Controller	Response (Y1)			Interaction (Y2)			Interaction (Y1)			Response (Y2)			Sum of ISE
	ISE	IAE	ITAE	ISE	IAE	ITAE	ISE	IAE	ITAE	ISE	IAE	ITAE	
Decentralized	1.341	2.128	3.809	0.2276	1.059	3.515	0.3412	1.292	4.272	1.323	2.086	3.671	3.2328
Centralized	1.195	1.726	2.522	0.09778	0.5731	1.646	0.0618	0.4697	1.401	1.19	1.681	2.236	2.54458

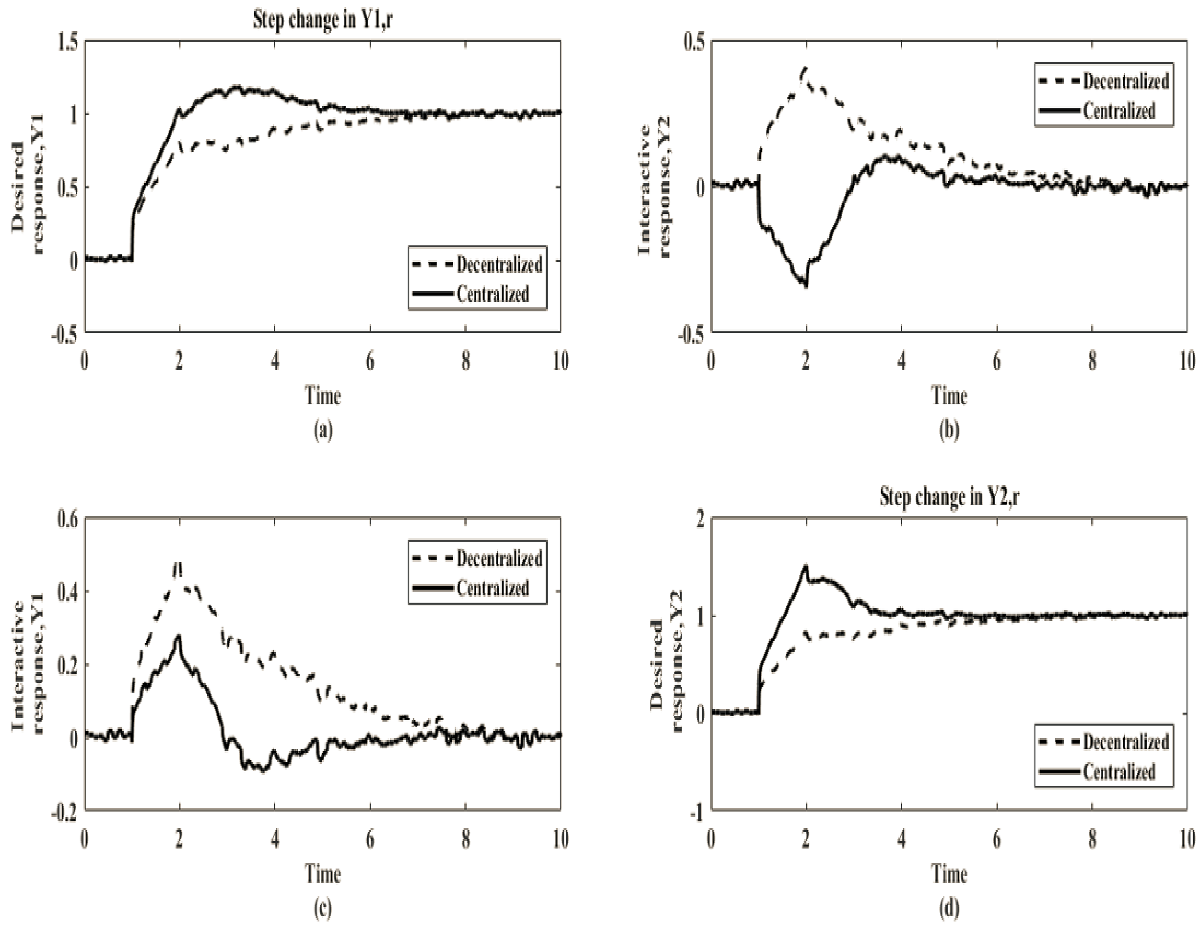

Fig. 17: Process and interaction curve of servo response in presence of random noise (Model 1).

Table 23: Relay feedback test results for decentralized control design with noise (Model 2).

h_1	h_2	h_3	a_1	a_2	a_3	P_{u1}	P_{u2}	P_{u3}
0.3	0.3	0.3	0.777	0.777	0.389	20.9	20.9	10.51

Table 24: PID controller parameters for decentralized controller with noise (Model 2).

	K_u	K_C	K_I	K_D
$G_{c,11}$	0.4915	0.2949	0.02822	0.7704
$G_{c,21}$	0.4915	0.2949	0.02822	0.7704
$G_{c,32}$	0.9819	0.5891	0.1121	1.2899

$\tau_{I1}= 10.45$; $\tau_{I2}= 5.255$; $\tau_{D1} = 2.6125$; $\tau_{D2} = 1.31375$

Table 25: Relay feedback test results for centralized control design with noise (Model 2).

h_1	h_2	h_3	h_4	h_5	h_6	a_1	a_2	a_3	a_4	a_5	a_6	P_u
0.4	0.3	0.4	-0.3	0.4	0.3	0.979	0.979	0.979	1.4	1.4	1.4	18.29

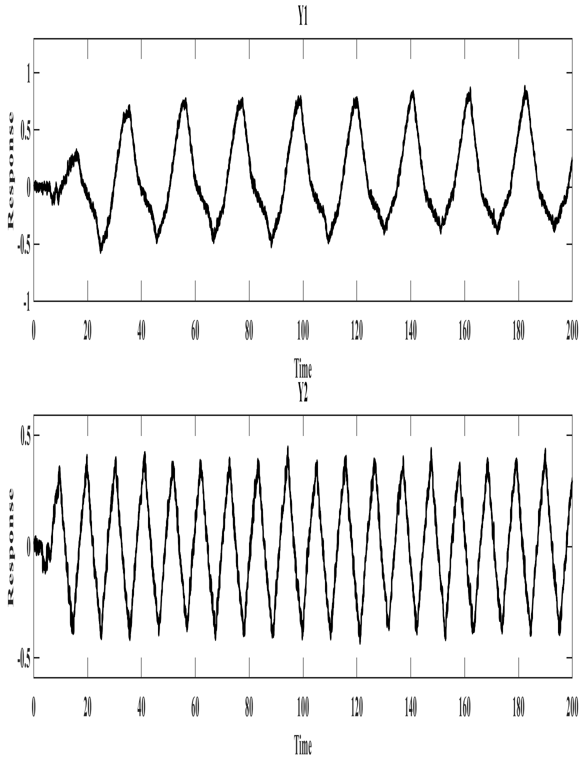

Fig. 18: Relay response for decentralized control design in presence of random noise (Model 2).

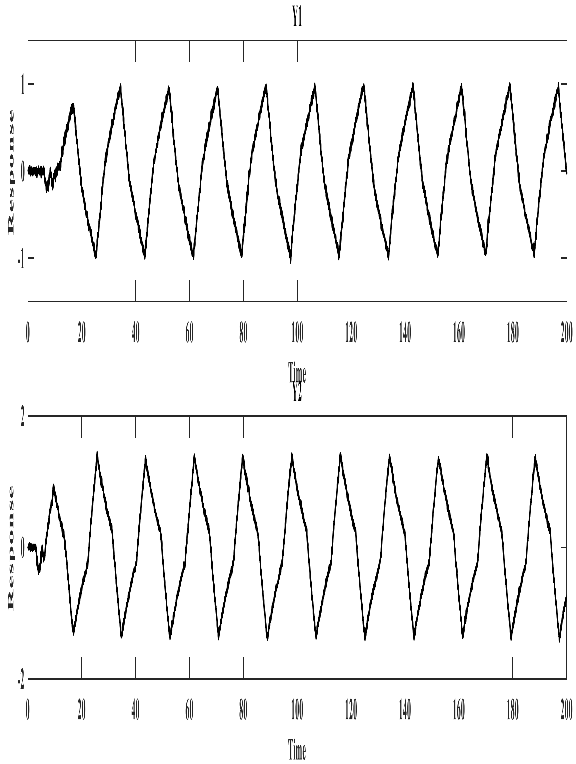

Fig. 19: Relay response for centralized control design in presence of random noise (Model 2).

The controller performance analysis of servo response with noise for Model 2 is listed in Table 27.

From Table 27, it is observed that there is an improvement in the time-integral analysis as the sum of ISE values of the decentralized control system is less than the centralized control system performance with the existence of noise.

CONCLUSIONS

The simultaneous relay autotuning method is proposed to design the decentralized and centralized PID controllers for a non-square stable 2×3 MIMO system. Higher-order harmonics are considered from the initial dynamics of the sustained relay response. The improved ultimate gains

Table 26: PID controller parameters for centralized controller with noise (Model 2).

	K_u	K_C	K_I	K_D	y(t*)	a*(N=3,1)	K_u*	K_C*
$G_{c,11}$	0.5202	0.3121	0.03412	0.7134	0.782	0.7038	0.7236	0.4341
$G_{c,12}$	0.3901	0.2340	0.0255	0.5349	0.782	0.7038	0.5427	0.3256
$G_{c,21}$	0.5202	0.3121	0.0341	0.7134	0.782	0.7038	0.7236	0.4341
$G_{c,22}$	-0.2728	-0.1637	-0.0179	-0.3742	1	0.9	-0.4244	-0.2546
$G_{c,31}$	0.3637	0.2182	0.0238	0.4988	1	0.9	0.5658	0.3395
$G_{c,32}$	0.2728	0.1637	0.0179	0.3742	1	0.9	0.4244	0.2546

τ_I = 9.145; τ_D = 2.286; ω_u= 0.3435; t=4.5729*

Table 27: Control performance analysis for servo response with noise (Model 2).

Controller	Response (Y1)			Interaction (Y2)			Interaction (Y1)			Response (Y2)			Sum of ISE
	ISE	IAE	ITAE	ISE	IAE	ITAE	ISE	IAE	ITAE	ISE	IAE	ITAE	
Decentralized	10.41	17.47	289.9	0.0498	1.386	41.74	2.158	7.144	135	3.486	6.228	67.33	16.463
Centralized	8.336	12.73	141.8	2.111	6.621	101.9	3.428	3.135	61.56	3.541	6.392	68.02	17.408

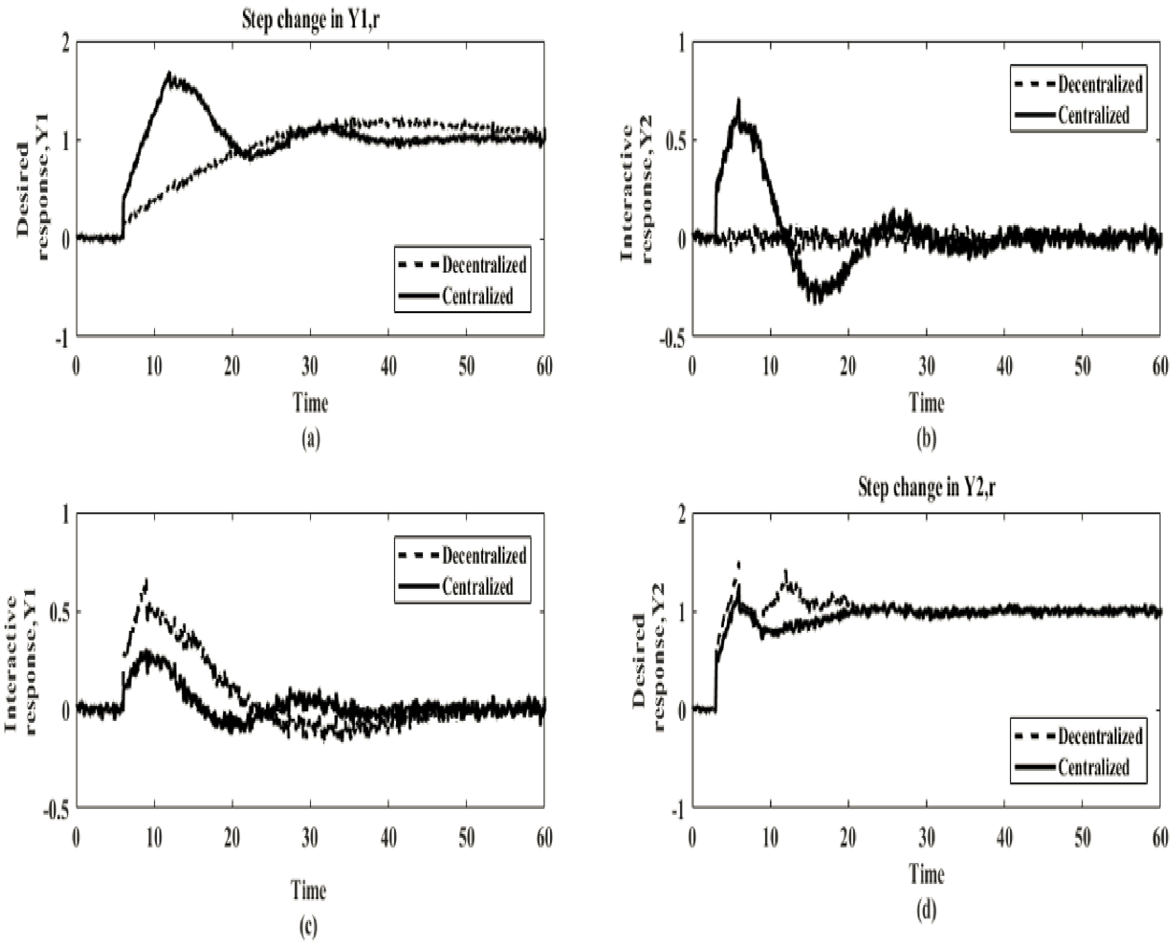

Fig. 20: Process and interaction curve of servo response in presence of random noise (Model 2).

are computed by incorporating HOH terms. Two non-square 2×3 MIMO transfer function models with different levels of interactions are considered for implementing the proposed work using simulation. The comparison performances of decentralized and centralized PID controllers using the simultaneous relay autotuning method are determined qualitatively and quantitatively. The ISE and IAE values of the non-square MIMO systems show a significant percentage improvement in performance and reduced interactions. Simulation of two examples of time integral analysis proves robustness and good control performance in the presence of measurement noise.

The RGA value obtained for Model 1 is greater than 1, which indicates that the system is highly interactive. In this case, the percentages of ISE values obtained for the centralized controller in servo response are 18% and 29%, and regulatory response are 19%, 19%, and 22% superior than the decentralized controller. However, the RGA value obtained for Model 2 is lesser than 1, which indicates that the system is less interactive. In this case, the percentage of ISE values obtained for the decentralized controller in servo response is 41% and the percentage of ISE values obtained for the centralized controller is 30%. For regulatory response, the ISE values obtained for the setpoint change in u1 is 28% for the decentralized control system, setpoint change in u2 is 14% for the centralized control system, and u3 is 31% for the decentralized control system. From the analysis, it is observed that when the system is highly interactive, the centralized control system provides a significant improvement over the decentralized control system, whereas when the system is less interactive, the decentralized control system provides a better improvement over the centralized control system.

Nomenclature

a	Amplitude of the relay
$G_c(s)$	Controller transfer function matrix
$G_p(s)$	Process transfer function matrix
h	Relay height
ISE	Integral Square Error
IAE	Integral Absolute Error
ITAE	Integral Time weighted Absolute Error
K_C	Controller gain
K_D	Derivative gain
K_I	Integral gain
K_p	Process gain
K_u	Ultimate gain
P_u	Period of oscillations ($=2\pi/\omega_u$)
t	Time
t*	$= 0.5\pi/\omega_u$
τ_i	Integral time
u_i	Manipulated variable
ω_u	Ultimate period of oscillations
y_i	Controlled variable
Λ	Block Relative Gain Array (BRG)

Acknowledgement

D. Kalpana gratefully acknowledges the Tamilnadu State Council for Science and Technology, Chennai for providing Young Scientist Fellowship to carry out collaborative research at National Institute of Technology, Warangal.

Received : Jan. 22, 2022 ; Accepted : Apr. 18, 2022

REFERENCES

[1] Ziegler J.G., Nichols N.B., Optimum Settings For Automatic Controllers, *Trans ASME*, **64**: 759-765 (1942).

[2] Yu C.C., "Autotuning of PID Controllers – A Relay Feedback Approach", 2nd ed, Springer-Verlag, London, (2006).

[3] Chidambaram M., Vivek Sathe., "Relay Auto Tuning for Identification and Control", Cambridge, Cambridge University Press, (2014).

[4] Chidambaram M., Nikita Saxena., "Relay tuning of PID controllers for Unstable MIMO systems", New Delhi, Springer, (2018).

[5] Palmor Z.J., Halevi Y., Krasne N., Automatic Tuning of Decentralized PID Controllers for TITO Processes, *Automatica*, **31(7)**: 1001-1010 (1995).

[6] Friman M., Waller K.V., Autotuning of Multiloop Control Systems, *Ind. Eng. Chem. Res*, **33(7)**: 1708-1717 (1994).

[7] Atherton D.P., Relay Autotuning: A Use of Old Ideas in a New Setting, *Transactions of the Institute of Measurement and Control*, **22(1)**: 103-122 (2000).

[8] Astrom K.J., Hagglund T., Automatic Tuning of Simple Regulators with Specifications on Phase and Amplitude Margins, *Automatica*, **20(5)**: 645–651 (1984).

[9] Luyben W.L., Derivation of Transfer Functions for Highly Nonlinear Distillation Columns, *Ind. Eng. Chem. Res*, **26(12)**: 2490–2495 (1987).

[10] Jietae Lee., Su Whan Sung., Friedrich Y. Lee., Michael Baldea., and Thomas F. Edgar., Full Closed-Loop Tests for the Relay Feedback Autotuning of Stable, Integrating, and Unstable Processes, *ACS Omega*, **4 (20)**: 18760−18770 (2019).

[11] Majhi S., Atherton D.P., Autotuning and Controller Design for Processes with Small Time Delays, IEEE Proceedings - *Control Theory Appl*, **146(5)**: 415–425 (1999).

[12] Thyagarajan T., Yu C.C., Improved Autotuning Using the Shape Factor from Relay Feedback, *Ind. Eng. Chem. Res*, **42(20)**: 4425–4440 (2003).

[13] Wang Q.G., Hang C.C., Zou B., Low-Order Modeling from Relay Feedback, *Ind. Eng. Chem. Res*, **36(2)**: 375-381 (1997).

[14] Panda R.C., Yu C.C., Analytical Expressions for Relay Feedback Responses, *Journal of Process Control*, **13(6)**: 489–501 (2003).

[15] Tao Liu., Furong Gao., Alternative Identification Algorithm for Obtaining A First-Order Stable/Unstable Process Model from Single Relay Feedback Test, *Ind. Eng. Chem. Res*, **47(4)**: 1140-1149 (2008).

[16] Srinivasan K., Chidambaram M., Modified Relay Feedback Method for Improved System Identification, *Computers & Chemical Engineering*, **27(5)**: 727-732 (2003).

[17] Huang H.P., Lee M.W., Tang Y.T., Identification of Wiener Model Using Relay Feedback Test, *Journal of Chemical Engineering Japan*, **31(4)**: 604-612 (1998).

[18] Shen S.H., Yu C.C., Use of Relay-Feedback Test for Automatic Tuning of Multivariable System, *AIChE Journal*, **40(4)**: 627–646 (1994).

[19] Panda R.C., Sujatha V., Parameter Estimation of Linear MIMO Systems Using Sequential Relay Feedback Test, *AIChE Journal*, **60(5)**: 1672-1681 (2014).

[20] Kalpana D., Thyagarajan T., Gokulraj N., Modeling and Control of Non-Square MIMO System Using Relay Feedback, *ISA Transactions*, **59**: 408-417 (2015).

[21] Reeves D.E., Arkun Y., Interaction Measures for Non-Square Decentralized Control Structure, *American Institute of Chemical Engineers Journal*, **35(4)**: 603-613 (1989).

[22] Valchos C., Williams D., Gomm J.B., Solution to the Shell Control Problem Using Genetically Tuned PID Controllers, *Control Engineering Practice*, **10(2)**: 151–163 (2002).

[23] Muske K., Young J., Grosdidier P., Tani S., Crude Unit Product Quality Control, *Computers & Chemical Engineering*, **15(9)**: 629-638 (1991).

[24] Saidi I., Touati N., Dhahri A., Soudani D., A Comparative Study on Existing and New Methods to Design Internal Model Controllers for Non-Square Systems, *Transactions of the Institute of Measurement and Control*, **41(13)**: 3637-3650 (2019).

[25] Chen J., He Z.F., Qi X., A New Control Method for MIMO First Order Time Delay Non-Square Systems, *Journal of Process Control*, 21(4): 538-546 (2011).

[26] Jin Q., Jiang B., Wang Q., Shan G., Decoupling Internal Model Control for Non-Square Processes Based on Equivalent Transfer Function, *Transactions of the Institute of Measurement and Control*, **36(8)**: 1114-1131 (2014).

[27] Lamara A., Colin G., Lanusse P., Chamaillard Y., Charlet A., Decentralized Robust Control-System for a Non-Square MIMO System, the Air-Path of a Turbocharged Diesel Engine, *IFAC Proceedings*, **45(30)**: 130–137 (2012).

[28] Luan X., Chen Q., Liu F., Centralized PI Control for High Dimensional Multivariable Systems Based on Equivalent Transfer Function, *ISA Transactions*, **53(5)**: 1554-1561 (2014).

[29] Quan L., Zhang H., Yang Y., A Novel Internal Model Control Method for Non-Square System, *Applied Mechanics and Materials*, **238**: 66-70 (2012).

[30] Rao S., Chidambaram M., Smith Delay Compensator for Multivariable Non-Square Systems with Multiple Time Delays, *Computers and Chemical Engineering*, **30(8)**: 1243–1255 (2006).

[31] Shinde D., Hamde S., Waghmare L., Predictive PI Control Multivariable Non-Square System with Multiple Time Delays, *International Journal for Science and Research in Technology*, **1(5)**: 26-29 (2015).

[32] Govindhakannan J., Chidambaram M., Multivariable PI Control of Unstable Systems, *Process Control Quality*, **10**: 319-329 (1997).

[33] Saxena Nikita., Chidamabram M., Relay Autotuning of Decentralized PID Controllers for Unstable TITO Systems, *Indian Chemical Engineer*, **60(1)**: 1- 15 (2016).

[34] Loh E.J., Chiu M.S., Robust Decentralized Control of Non Square Systems, *Chemical Engineering Communications*, **158(1)**: 157-180 (1997).

[35] Sujatha V., Panda R.C., Time Domain Modeling and Control of Complex Non-Linear Chemical Processes Using Relay Feedback Test, *Transactions of the Institute of Measurement and Control*, **42(15)**: 2885-2907 (2020).

[36] Kalpana D., Chidambaram M., Auto Tuning of Decentralized PI Controllers for a Non-Square Unstable MIMO System, *In 2020 First IEEE International Conference on Measurement, Instrumentation, Control and Automation (ICMICA)*, 1-5, IEEE, (2020).

[37] Kalpana D., Chidambaram M., Auto-tuning of Decentralized PI Controllers for a Non-Square System, *Advances in Automation, Signal Processing, Instrumentation, and Control: Select Proceedings of I-CASIC 2020*, **700**: 253-259 (2021).

[38] Priyadharsini M., Kalpana D., Chidambaram M., "AutoTuning of Centralized PID Controllers for a Non-square Unstable MIMO System", *3rd International Conference on Innovations in Power and Advanced Computing Technologies (i-PACT)*, 1-5 IEEE, (2021).